

Article

Application of Deep Learning Algorithm in Optimization Control of Electrostatic Precipitator in Coal-Fired Power Plants

Jianjun Zhu ¹, Chao Feng ^{1,*}, Zhongyang Zhao ², Haoming Yang ¹ and Yujie Liu ¹

¹ Zhejiang Doway Advanced Technology Co., Ltd., Jinhua 321000, China; mrjianjun28@163.com (J.Z.); yanghaoming0115@163.com (H.Y.); liuyj9009@163.com (Y.L.)

² State Key Laboratory of Clean Energy Utilization, State Environmental Protection Center for Coal-Fired Air Pollution Control, Zhejiang University, Hangzhou 310058, China; 11827067@zju.edu.cn

* Correspondence: stevenxut@163.com

Abstract: The new energy structure needs to balance energy security and dual carbon goals, which has brought major challenges to coal-fired power plants. The pollution reduction and carbon emissions reduction in coal-fired power plants will be a key task in the future. In this paper, an optimization technique for the operation of an electrostatic precipitator is proposed. Firstly, the voltage-current model is constructed based on the modified dust charging mechanism; the modified parameters are trained through the gradient descent method. Then, the outlet dust concentration prediction model is constructed by coupling the mechanism model with the data model; the data model adopts the long short-term memory network and the attention mechanism. Finally, the particle swarm optimization algorithm is used to achieve the optimal energy consumption while ensuring stable outlet dust concentration. By training with historical data collected on site, accurate predictions of the secondary current and outlet dust concentration of the electrostatic precipitator have been achieved. The mean absolute percentage error of the voltage-current characteristic model is 1.43%, and the relative root mean-squared error is 2%. The mean absolute percentage error of the outlet dust concentration prediction model on the testing set is 5.2%, and the relative root mean-squared error is 6.9%. The optimization experiment is carried out in a 330 MW coal-fired power plant. The results show that the fluctuation of the outlet dust concentration is more stable, and the energy saving is about 43% after optimization; according to the annual operation of 300 days, the annual average carbon reduction is approximately 2621.34 tons. This method is effective and can be applied widely.

Keywords: pollution reduction; carbon emissions reduction; long short-term memory; attention mechanism; energy saving; concentration prediction; particle swarm optimization



Citation: Zhu, J.; Feng, C.; Zhao, Z.; Yang, H.; Liu, Y. Application of Deep Learning Algorithm in Optimization Control of Electrostatic Precipitator in Coal-Fired Power Plants. *Processes* **2024**, *12*, 477. <https://doi.org/10.3390/pr12030477>

Academic Editors: Zhiwei Gao and Wen-Jer Chang

Received: 13 January 2024

Revised: 23 February 2024

Accepted: 24 February 2024

Published: 27 February 2024



Copyright: © 2024 by the authors. Licensee MDPI, Basel, Switzerland. This article is an open access article distributed under the terms and conditions of the Creative Commons Attribution (CC BY) license (<https://creativecommons.org/licenses/by/4.0/>).

1. Introduction

In the context of dual carbon, renewable energy generation has increased steadily, the proportion of coal power installed capacity has continued to decline, and the role of coal-fired power plants as a foundational and system-regulating power source is also becoming increasingly clear [1]. However, from the perspective of security and energy security, it is difficult to fundamentally change the energy structure dominated by coal in a short time. The new energy structure needs to take into account energy security and dual carbon goals [2]. The effective collaborative development of coal power and new energy is the key to building a new power system and ensuring energy security and stability, which brings major challenges to coal-fired power plants, mainly including frequent start-up and large load change, deep peak regulation, and biomass blending [3–5].

In response to these challenges, coal-fired power plants have adopted a series of measures, including optimizing the operation mode, improving the energy utilization efficiency, and developing carbon capture and storage technology [6]. As the main device for particulate matter removal, an electrostatic precipitator (ESP) directly affects the reduction

effectiveness of pollution and carbon emissions in coal-fired power plants. An ESP realizes dust removal by consuming energy; the greater the energy consumption, the higher the dust removal efficiency [7–9]; therefore, in order to ensure the outlet dust concentration meets the standard, the operation energy consumption of an ESP in coal-fired power plants is generally high [10]. In addition, the fuel composition and operating conditions have become more complex due to factors such as biomass blending, deep peaking, and fuel cost, which puts new requirements on the stable operation of an ESP. Therefore, it is urgent to develop the optimization operation technology of an ESP to reduce pollution and carbon emissions, so as to achieve ultra-low emissions of PM under complex working conditions while reducing energy consumption.

An ESP is generally optimized by negative feedback on the outlet dust concentration, which cannot take into account the mutual influence of each electric field and cannot achieve the optimal solution. For the optimization of an ESP, a large number of scholars have carried out relevant research. Li et al. [11] proposed a least square fitting model to identify the corona power of an ESP, using the neural network model to predict the outlet dust concentration and using a genetic algorithm to achieve optimal control. Chen Weiguang [12] built a mathematical model for an ESP and proposed an optimization control method based on fuzzy logic and multi-objective programming. Grass [13] et al. proposed a fuzzy control strategy to adjust the ESP by boiler load dynamically. Liu et al. [14] studied the influence of different high-voltage power supplies and power supply modes on outlet dust concentration, analyzed power consumption under different working conditions, and proposed optimization operation strategies under different working conditions. In order to achieve the optimal control, power consumption and outlet dust concentration must be accurately obtained.

The above research has achieved certain results. However, the temporal correlation between the input and output of an ESP has not yet been considered, and the lack of critical information makes it impossible to build an accurate prediction model. The movement of flue gas from the inlet to the outlet of the ESP takes time, and the outlet dust concentration has a time delay relative to the flue gas parameters and power parameters. The outlet dust concentration is the result of the combined effects of relevant parameters over a period of time; therefore, it is necessary to choose an algorithmic model that takes temporal correlation into consideration. The long short-term memory (LSTM) network can solve the problem of gradient disappearance or explosion in the recurrent neural network and has long-term memory capabilities, making it very suitable for processing long-term response data. Moreover, most of the ESPs in coal-fired power plants consist of multiple chambers and multiple electric fields. Considering factors such as structural differences, wear of wire, change in operating conditions, flue gas flow field, fuel characteristics, and the characteristics of each field are independent and correlated, there are still some problems that need to be solved.

In this paper, the affecting factors are analyzed, and the voltage-current characteristic model and the outlet dust concentration prediction model are established. Through the prediction results of the voltage-current characteristic model and the outlet dust concentration prediction model, the particle swarm optimization (PSO) algorithm is used to obtain the optimal secondary voltage under the requirement of satisfying the outlet dust concentration. Finally, an optimization experiment is carried out in a 330 MW coal-fired power plant.

The rest of this paper is as follows. Section 2 proposes an optimization control method and discusses the affecting factors; Section 3 analyzes the results of the optimization control method; and Section 4 is the conclusion of this paper.

2. Main Affecting Factors and Control Methods

The optimization control of an ESP is a complex engineering system with multiple inputs and outputs, strong coupling, and is nonlinear and hysteretic with dynamic changes [15]. As shown in Figure 1, the ESP in a 330 MW power plant consists of four cham-

bers (Chamber A1–B2) connected in parallel and five electric fields (Field 1–5) connected in series, which is highly sensitive to multiple variables.

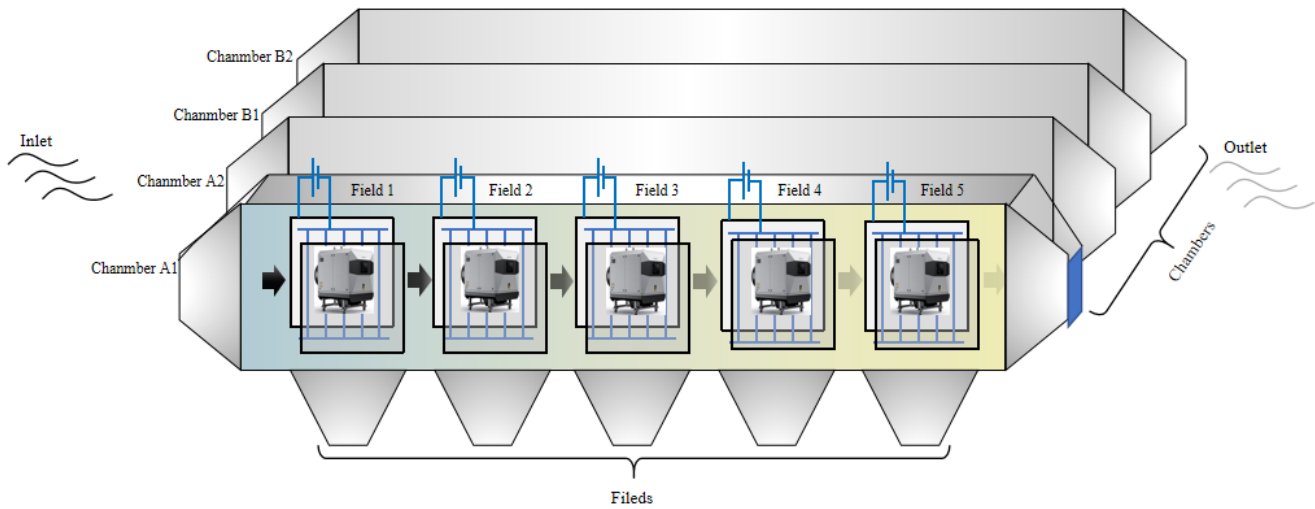


Figure 1. Structure of an ESP in a 330MW power plant.

2.1. Main Affecting Factors

Load and coal. The load is dynamically variable, and the current coal composition is relatively complex. Due to the fixed mechanical structure, the inlet flue gas volume varies with load and coal. When the flue gas volume is large, the flue gas flow rate is fast, and the flue gas residence time in the chamber is short, which will reduce the overall dust removal efficiency. Therefore, the input power of the electric field can be adjusted according to the change in the load and coal.

Mechanical structure. An ESP consists of multiple chambers connected in parallel and multiple electric fields connected in series. Under normal circumstances, the deviation of each chamber is very small, and the channels are independent of each other, so we only need to analyze a single chamber. The dust removal efficiency of a single chamber depends on the dust removal efficiency of each electric field within the chamber, and the overall dust removal efficiency is the average of the dust removal efficiencies of all the chambers. The dust removal efficiency is closely related to each electric field. The dust removal efficiency of an ESP can be calculated as follows:

$$\eta = \sum_{i=0}^n \eta_i / n \quad (1)$$

$$\eta_i = 1 - \prod_{j=1}^m (1 - \eta_{(i,j)}) \quad (2)$$

where η is the dust removal efficiency of ESP. η_i is the dust removal efficiency for chamber i . n is the total number of chambers. η_{ij} is the dust removal efficiency for chamber i and field j . m is the total number of electric fields in a single chamber.

High voltage. High voltage is applied to the discharge electrode to generate a strong electric field, and the gas will be ionized. Electrons are emitted into the gas layer near the corona electrode surface, and the dust particles in the flue gas gain charge through collision and diffusion and become charged particles. Under the action of the electric field force, these charged particles move to the collecting electrode and attach to the anode plate, so that the dust particles can be separated from flue gas [16]. The charging of particles and the driving speed of charged particles are both related to the voltage of the power supply. However, maintaining an excessively high voltage will result in significant corona current and energy waste. Therefore, different electric fields require a reasonable distribution of secondary voltage.

Rapping system. Charged particles lose charge and become neutral particles after reaching the collecting electrode, which is grounded, and then the collecting electrode is cleaned through mechanical rapping; in this way, the neutral particles will fall off. Therefore, setting a reasonable rapping time can better remove particulate matter. In addition, in order to ensure that the outlet dust concentration is up to standard, two electric fields cannot be simultaneously rapped in a common chamber.

2.2. Control Methods

The ESP is highly sensitive to multiple variables; the former fields will also have influence on the latter electric fields, so it is difficult to realize an accurate description with the mechanism. In order to achieve efficient pollutant reduction and low-cost operation, an optimization method for an ESP is designed, including the voltage-current characteristic model, the outlet dust concentration prediction model, and the PSO model. The voltage-current characteristic model is built based on the dust charging mechanism and the historical operating data of an ESP; the secondary current of an ESP can be calculated by the voltage-current characteristic model. Once the conversion efficiency of the power supply is given, the energy consumption can be calculated from the secondary voltage and secondary current. The outlet dust concentration prediction model is divided into two parts: firstly, the mechanism model is built based on the dust removal mechanism and the parameter correction method to obtain the predictive value of the mechanism model; secondly, the data model is built by a deep learning algorithm, which utilizes the historical data as input and the difference between the predictive value of the mechanism model and the measured value as output. The outlet dust concentration prediction is realized through the coupling of the mechanism with data. The PSO model derives the optimal secondary voltage based on the real-time operating conditions to minimize the energy consumption and to ensure compliance with emission standards.

2.2.1. Voltage-Current Characteristic Model

During the operation process, the operating cost of the ESP mainly considers the power consumption of the power supply. Therefore, it is only necessary to consider the power consumption of the power supply. The variation of the secondary voltage and secondary current causes changes in the power consumption, and the variation of the secondary voltage and secondary current is coupled according to the characteristics of the corona discharge. Under different secondary voltages, the current density is affected by parameters such as the flue gas composition and the electrode configuration; the secondary current can be obtained from the following equation [17]:

$$I_o = \frac{\varepsilon_0 b_i l}{16 s_y} [\gamma + \sqrt{\gamma^2 + 192(U_o - U_c)(s_y E_1)^3}] \quad (3)$$

$$\gamma = 9(U_o - U_c + s_y E_1)^2 - 12(s_y E_1)^2 \quad (4)$$

$$U_c = r_d E_0 \delta (\rho_i + 0.03 \sqrt{\frac{\rho_i}{r_d}}) \ln \frac{r_{eff}}{r_d} \quad (5)$$

$$E_1 = \frac{\pi U_c}{d_w \ln \frac{r_{eff}}{r_d}} \quad (6)$$

where ε_0 is the dielectric constant in vacuum. b_i is the ion mobility ($\text{cm}^2/\text{V}/\text{s}$). l is the total length (m) of the wire. s_y is the wire-plate distance (m). E_1 is the effective electric field intensity (V/m). U_o is the secondary voltage (V). U_c is the inception voltage (V). r_d is the radius (m) of the wire. E_0 is the electric field intensity (V/m) of the spark discharge under standard conditions. δ is the surface roughness of the discharge electrode. ρ_i is the relative density of the flue gas. r_{eff} is the effective cylinder radius (m). d_w is the wire-wire distance (m).

In the actual operation of an ESP, factors that affect the corona discharge include the accumulation of dust on the electrode plates and wires, wear and tear, the corona

enclosure, etc. The corona discharge process deviates from the ideal process described by Equation (3); the voltage-ampere characteristics are variable, the secondary voltage is proportional to the load when the secondary current is fixed, and there is a certain deviation between the effective secondary voltage and the operating secondary voltage. Therefore, it is necessary to modify the discharge mechanism model to improve its accuracy. This paper introduces some correction parameters into the corona discharge mechanism and calculates the effective discharge voltage using the following equation, based on the research results of Guo [18]:

$$U_o^* = U_o + \alpha L + \beta \quad (7)$$

where U_o^* is the effective secondary voltage (V). L is the load (MW). α and β are the correction factors.

The surface roughness of the discharge electrode, relative density of the flue gas, and ion migration rate all vary with the theoretical design parameters, which are also set as trainable variables. Subsequently, TensorFlow is used to construct the voltage-current characteristic correction model. This model takes coal, the secondary voltage of the power supply, and temperature as inputs and the secondary current as outputs. The model accuracy is improved through gradient descent training.

The energy consumption of an ESP can be described by the following equation:

$$P = U_o I_o / \eta_p \quad (8)$$

where η_p is the efficiency of the energy conversion from the primary side to the secondary side, $\geq 90\%$.

2.2.2. Outlet Dust Concentration Prediction Model

1. Mechanism model

The migration and removal processes of particles are affected by some factors, such as the mechanical parameters, flue gas parameters, and operational parameters of the power supply. It is generally believed that the removal of particles with different sizes is independent of each other, and there is no conversion between different sizes. The outlet dust concentration can be described by the following equation [19]:

$$C_o = \int_{d_{pmin}}^{d_{pmax}} C_o(d_p) dd_p \quad (9)$$

$$C_o(d_p) = C_{in}(d_p) \prod_{i=1}^n e^{n_{de}} \quad (10)$$

$$n_{de} = -\frac{A q(d_p, u_i) E(u_i) C_m(d_p)}{Q 3\pi\mu d_p} \quad (11)$$

where d_p , d_{pmin} , and d_{pmax} are the particle diameter (μm), minimum particle diameter (μm), and maximum particle diameter (μm), respectively. $C_{in}(d_p)$ and $C_o(d_p)$ are the dust concentration (mg/Nm^3), with the particle diameter of d_p at the inlet and outlet of the ESP, respectively. n is the total number of electric fields. n_{de} is the Deutsch number. $q(d_p, u_i)$ is the electrical charge (C) of the particle diameter of d_p in field i ; the particle charge is decided by the particle diameter and secondary voltage. $E(u_i)$ is the electric field intensity (V/m) of field i . $C_m(d_p)$ is the Cunningham correction factor for different particle diameters. A is the collecting plate area (m^2) of a single electric field. Q is the flue gas quantity (m^3/s). μ is the flue gas viscosity ($\text{Pa}\cdot\text{s}$).

Considering the deviation of the ideal process, according to the research [20] of Li et al., proportional and exponential factors are applied to correct the Deutsch number. The corrected outlet dust concentration equation is given as:

$$C_o = \int_{d_{pmin}}^{d_{pmax}} C_{in}(d_p) \prod_{i=1}^n e^{f(n_{de})} dd_p \quad (12)$$

$$f(n_{de}) = \lambda_1 n_{de}^{\lambda_2} \tag{13}$$

where λ_1 is the proportional factor and λ_2 is the exponential factor.

2. Data model

The mechanism model has now been constructed, but it still has some defects. Therefore, the data model needs to be built. By utilizing the mechanism model, the difference between the predictive outlet dust concentration and the measured value can be obtained, and the difference will be used as the target value in the data model. In this way, a mechanism-and-data-coupled outlet dust concentration prediction model is constructed; the model has the advantages of high accuracy and generalization ability.

Due to the time required for the flue gas to flow from the inlet to the outlet, the historical data of coal, flue gas, and power-related parameters are refreshed in seconds. The outlet dust concentration is lagging behind, which is the result of the effects of relevant parameters during the period from the inlet to the outlet of flue gas. When using time series data for regression modeling, it is possible to consider the impact of input from multiple time steps on the output. In this paper, the LSTM network is used in the data model; since the dust removal process involves many parameters, the attention mechanism is added into the LSTM (A-LSTM) network. The attention mechanism selectively filters a small amount of key information from a large amount of data and effectively highlights the importance of different parameters, and the accuracy and generalization ability of the model can be improved [21]. The A-LSTM network structure is displayed in Figure 2.

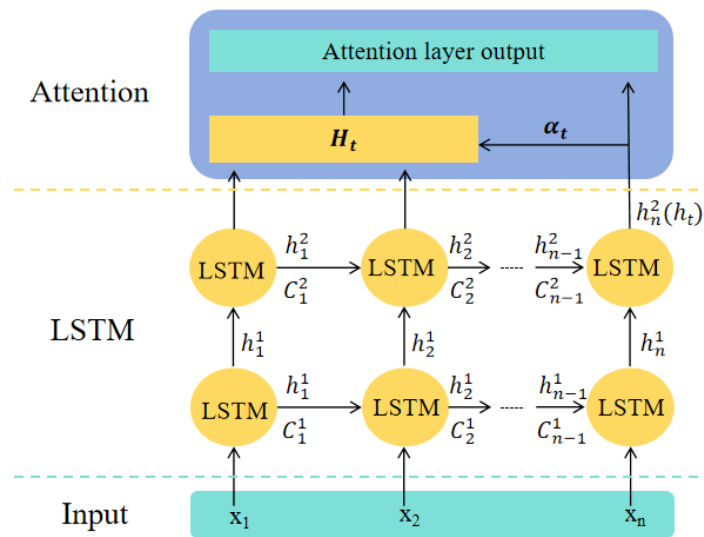


Figure 2. A-LSTM network structure of the data model.

The attention layer is used to process the time series data output by the LSTM layer and can be represented by the following equation:

$$s_t = \text{softmax}(h_t^T W^k h_{all}) \tag{14}$$

$$H_t = \sum_{t=1}^n s_t h_n \tag{15}$$

$$y = \tanh(W_c [H_t; h_t]) \tag{16}$$

where h_t is the hidden state of the last LSTM layer output at the last moment. h_{all} is the hidden state of the last LSTM layer output. W^k is the weight matrix. s_t is the coefficient vector. $\text{softmax}()$ and $\tanh()$ are the activation functions. n is the time step of the LSTM network. H_t is the temporal weight vector. W_c is the temporal weight matrix. y is the output of the A-LSTM.

In the data model, air volume, secondary voltage of the power supply, inlet temperature of the ESP, and coal are used as inputs, while dust concentration deviation is used as

the output. The root mean square error (RMSE) is used as the evaluation function for the model, and RMSE is calculated as follows:

$$y_i = C_{o,i} - C'_{o,i} \quad (17)$$

$$RMSE = \sqrt{\frac{1}{n} \sum_{i=1}^n (y_i - y'_i)^2} \quad (18)$$

where $C_{o,i}$ is the measured value (mg/Nm^3) of number i . $C'_{o,i}$ is the predictive value (mg/Nm^3) of number i in the mechanism model. y'_i is the predictive value (mg/Nm^3) of number i in the data model.

2.2.3. PSO Model

The optimization goal of an ESP is to minimize the operational cost by providing each electric field with a secondary voltage while meeting the outlet dust concentration standards. The optimization operation is a nonlinear programming problem, which can be effectively solved by PSO due to its advantages in searching and optimizing nonlinear systems in multiple dimensions. PSO is suitable for the optimization of an ESP. When using PSO to construct the optimization control problem, the total energy consumption of an ESP should be minimized while meeting the emission limit, which can be expressed as:

$$\min \sum_{i=1}^n P_i \quad (19)$$

$$\text{s.t.} \begin{cases} c'_{out} \leq c_{limit} \\ u_{i,min} \leq u_i \leq u_{i,max} \end{cases} \quad (20)$$

where n is the total number of electric fields. P_i is the power (kW) of field i . c'_{out} and c_{limit} are the predictive value (mg/Nm^3) and limit value (mg/Nm^3) of the outlet dust concentration, respectively. u_i , $u_{i,min}$, and $u_{i,max}$ are the secondary voltage (kV), minimum secondary voltage (kV), and maximum secondary voltage (kV) of field i , respectively.

There are constraints in this optimization problem. Generally, the way to solve constrained optimization problems is to construct penalty functions, which incorporate the boundary conditions into the objective function of the optimization problem, thereby creating a new objective function. The solution to the original optimization problem is obtained by solving the new optimization problem. There are several penalty functions that can be used when particles are outside the boundary conditions; for instance, the dead penalty function sets the fitness of particles to infinity directly, the static penalty function gives particles a fixed punishment, and the hierarchical penalty function [22] adopts different penalty coefficients based on the degree of violation of the penalty function. In this article, the A-LSTM network is used to correct the dynamic characteristics of an ESP, and the trend of the dust concentration changes at the outlet can be calculated with a few steps. Therefore, the following form of hierarchical penalty function is adopted:

$$Penalty = \varepsilon \sum_{i=1}^m \frac{\text{sgn}(c'_{out,i} - c_{limit}) + 1}{2} \quad (21)$$

where m is the total step. ε is penalty coefficient. $\text{sgn}()$ is the signum function. $c'_{out,i}$ is the predictive value (mg/Nm^3) of the outlet dust concentration at step i .

This form of the penalty function imposes a higher penalty on particles that exceed the limit many times; the optimization problem can then be described as:

$$\min \sum_{i=1}^n P_i + Penalty \quad (22)$$

$$\text{s.t.} u_{i,min} \leq u_i \leq u_{i,max} \quad (23)$$

Obviously, the above problem is a nonlinear programming problem, which cannot be solved using conventional linear programming methods. Therefore, the PSO algorithm is

adopted to solve the above problem. According to the principles of the PSO algorithm, the secondary voltage is abstracted as the position attributes of particles, which are randomly generated within the solution space, and Equation (22) is the fitness function. The position and velocity of the particles can be updated based on their fitness, according to the following equation:

$$V_{i,t+1} = \omega V_{i,t} + c_1 r_1 (P_{i,pbest} - P_{i,t}) + c_2 r_2 (P_{gbest} - P_{i,t}) \quad (24)$$

$$P_{i,t+1} = P_{i,t} + V_{i,t+1} \quad (25)$$

where ω is the inertia weight. $V_{i,t}$ is the velocity vector of particle i at time t . C_1 and C_2 are the learning factors. r_1 and r_2 are the random numbers. $P_{i,pbest}$ is the optimal position vector in the history of the particle. P_{gbest} is the global optimal position vector of all the particles. $P_{i,t}$ is the position vector of particle i at time t .

When using TensorFlow to run the PSO model, some parameters need to be set. The specific parameters are set as follows: the particle number is 50; the iteration number is 10; the mode is vectorization; the upper value is 80; the lower value is 30; the inertia weight is 0.8; the learning factors are 0.5.

Figure 3 shows the PSO process of an ESP; the information contained in the particles correspond to the secondary voltage of each electric field. The PSO process can be described as follows: (1) Logical judgment, which ensures that the emissions are controlled within the limit values under various operating conditions; it is reasonable to set the target value at 80% of the limit value. (2) Particle initialization, the purpose of particle initialization is to set the initial secondary voltage for the particle swarm, and the secondary voltage value must be within the allowable range of the device. (3) Fitness calculation. (4) Update the global best particle and continue to calculate fitness and update the particle until the end of iteration. (5) End the current optimization. This process needs to be used repeatedly in practical work in order to ensure the reliable and stable operation of the system; it is also necessary to consider factors such as severe fluctuations in operating conditions, secondary dust caused by rapping, and distortion of the turbidity meter.

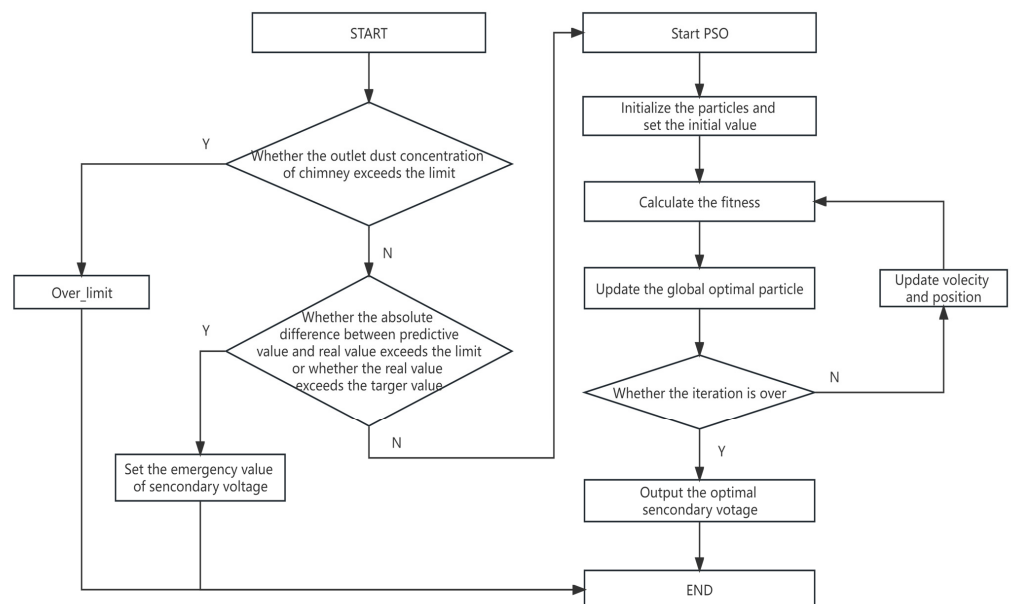


Figure 3. PSO process of an ESP.

3. Results

In order to validate the effectiveness of the optimization control, the research is conducted on the ESP of a 330 MW power plant, and each electric field is equipped with an independent high-voltage power supply. The detailed design parameters are shown in Table 1. The optimization system contains a prediction module, an optimization module,

and a control module. The prediction and optimization modules are developed based on the Python platform, and the control module communicates with external systems through the OPC protocol.

Table 1. Design parameters of an ESP.

Design Parameter	Unit	Value
effective cross-sectional area	m ²	276
effective length	m	3.91
specific collecting area	m ² /(m ³ /s)	106.42
flue gas velocity	m/s	0.87
wire-plate distance	m	0.2
wire-wire distance	m	0.49
discharge electrode type		field 1, 2, 3: barbed wire field 4, 5: spiral wire

3.1. Prediction Results and Analysis of Voltage-Current Characteristic Model

The secondary current prediction performance of the voltage-current characteristic model is shown in Figure 4. During the sampling period, the actual secondary current ranges from 100 mA to 1500 mA and covers almost all the operation conditions. The average value of the secondary current is 631 mA, the mean absolute error (MAE) is 9 mA, the mean absolute percentage error (MAPE) is 1.43%, the RMSE is 12 mA, the relative root mean-squared error (RRMSE) is 2%, R-squared (R2) is 0.98, and the maximum predictive deviation is 86 mA. Compared to the front electric fields (field 1–3), the relative deviation of the fourth and fifth electric fields is larger, with a MAE of 11 mA and a RMSE of 13.5 mA. This is because the discharge electrode type of the last two electric fields is a spiral wire and adopts the structure of one plate with two wires, which can produce a larger secondary current under the same secondary voltage; the average value of last two electric fields is 701 mA. The results show that a voltage-current characteristic model can accurately follow the change in the secondary current.

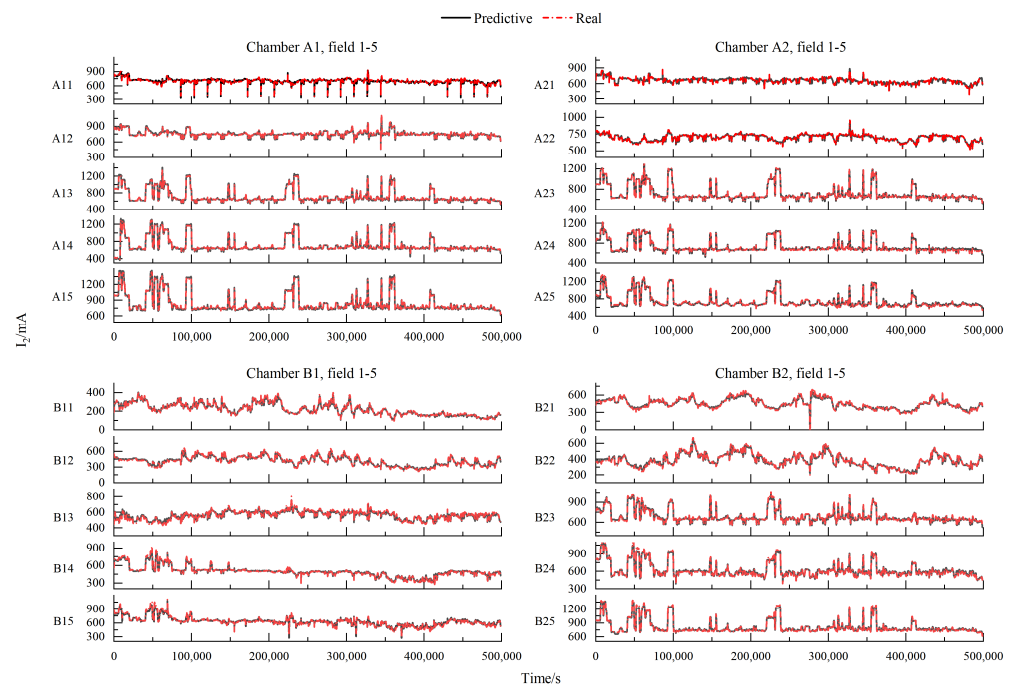


Figure 4. Comparison between predictive values and real values of secondary current.

3.2. Prediction Results and Analysis of Outlet Dust Concentration Prediction Model

With the mechanism model, it is difficult to eliminate impermeable disturbances such as airflow distribution and wear of the wire. The model adopts the fusion of mechanism and data; firstly, it predicts the outlet concentration by the modified mechanism model, and then it constructs the data model to calculate the deviation to obtain the prediction of the outlet dust concentration coupled with the mechanism and data. We constructed a data set using 500,000 historical data from the ESP; 85% of the data is selected as the training set, and the remaining 15% is used as the testing set. The result of the dust concentration prediction model on the training set is shown in Figure 5.

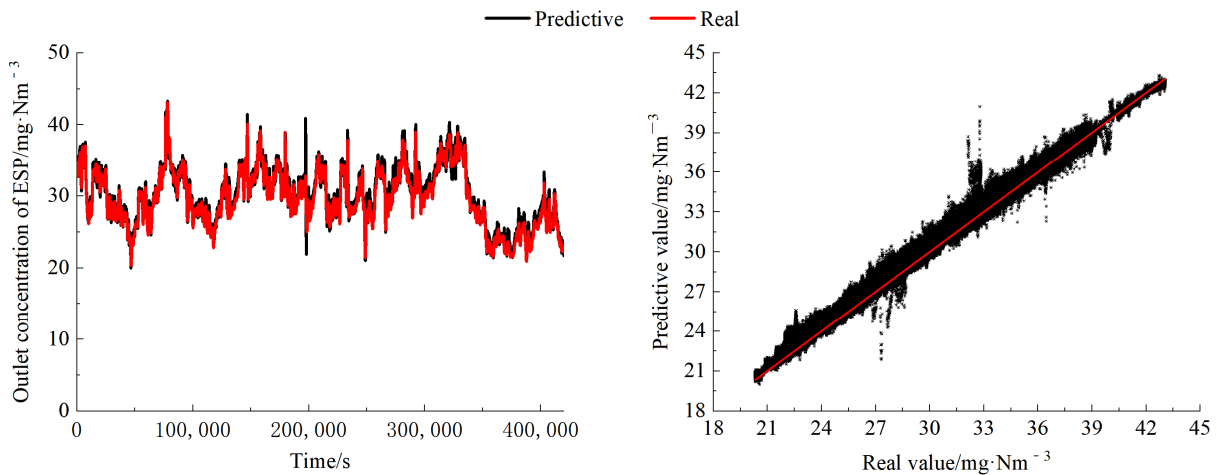


Figure 5. Result of outlet dust concentration prediction model on the training set.

The outlet dust concentration of the training set is distributed in the range of 20–45 mg/Nm³, and the average outlet dust concentration is 30.1 mg/Nm³. As shown in Figure 5, the prediction performance of the outlet dust concentration prediction model is outstanding; the MAE of the prediction is 0.43 mg/Nm³, the MAPE is 1.4%, the RMSE is 0.546 mg/Nm³, the RRMSE is 1.8% and the R² is 0.98. The prediction accuracy is high across the entire range of data, and the predictive values align with the real values in terms of trends. However, a well-fitted performance on the training set often leads to overfitting, which will reduce the generalization ability of the model. Therefore, it is necessary to observe the performance of the data model on the testing set. The result of the outlet dust concentration prediction model on the testing set is shown in Figure 6.

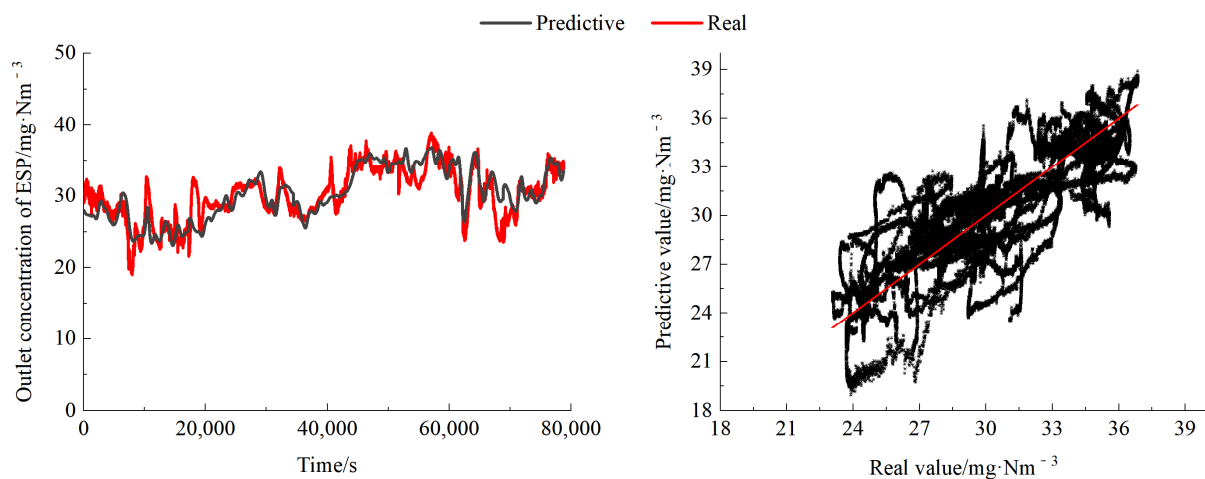


Figure 6. Result of outlet dust concentration prediction model on the testing set.

Figure 6 presents the performance of the outlet dust concentration prediction model on the testing set. The average value of the outlet dust concentration is 30.19 mg/Nm^3 , the MAE is 1.57 mg/Nm^3 , the MAPE is 5.2%, the RMSE is 2.08 mg/Nm^3 , the RRMSE is 6.9% and the R^2 is 0.66. As can be seen in Figure 6, the prediction of outlet dust concentration is relatively evenly distributed on both sides of the real value; according to the dimensionless evaluation indicators of the RRMSE and MAPE, the model has achieved an accurate outlet dust concentration prediction.

3.3. Prediction Results and Analysis of PSO Model

In order to validate the optimization performance of the PSO model, a comparative experiment is conducted in a 330 MW coal-fired power plant; manual control and PSO control are performed at similar conditions. The coal feeding quantity, total air volume, outlet dust concentration of the ESP, and the outlet dust concentration of chimney and energy consumption are shown in Figure 7.

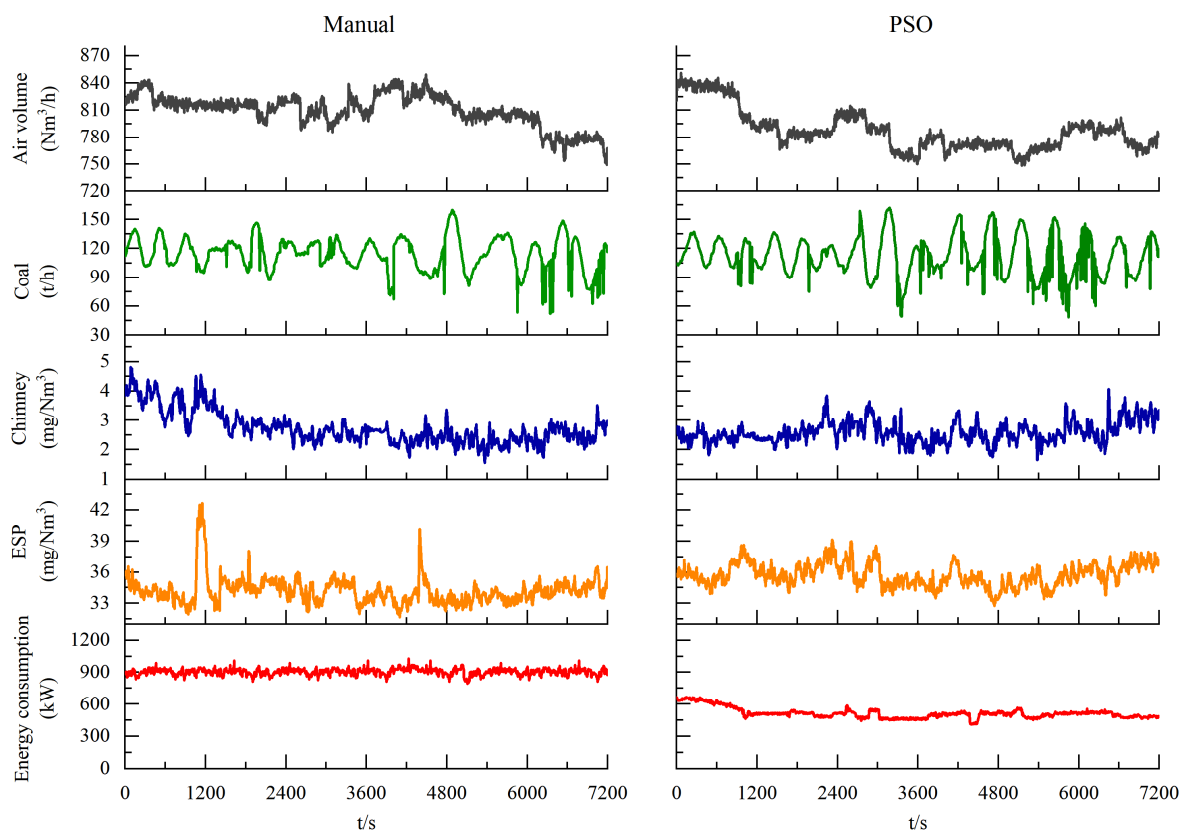


Figure 7. Comparison results before and after optimization.

When controlling manually, the secondary voltage is adjusted according to the experience of the operators and is usually set high due to efficiency requirements. In order to ensure the stable compliance of the outlet dust concentration, the secondary voltage is near the flashover point. At this moment, the energy consumption of the ESP is relatively high, with an average consumption of 904.46 kW ; the phenomenon of flashover coexists simultaneously, which can lead to an unstable outlet dust concentration. The average outlet dust concentration is 34.2 mg/Nm^3 , the maximum value is 42.6 mg/Nm^3 , and the minimum value is 31.6 mg/Nm^3 . After the PSO control, the energy consumption of the ESP significantly decreases, with an average energy consumption of 514.75 kW ; since the secondary voltage is much lower than before, there is almost no flashover. Moreover, when the input parameters are varied over a wide range, the outlet dust concentration becomes more stable, with fluctuation within $\pm 3 \text{ mg/Nm}^3$. Compared to the manual control, the

energy saving is about 43% after the PSO control. According to the annual operation of 300 days, the annual average carbon reduction is approximately 2621.34 tons.

3.4. Future Prospects

In this paper, some progress has been made in the research on the optimization of an ESP, and industrial validation has been carried out, but there are still some problems to be explored in the future:

- (1) An ESP can be primarily classified into dry and wet types. A wet ESP is generally installed after wet flue gas desulfurization to further remove the escaped ultra-fine particles, but due to its complex working process, there has been less research and development on its capture and optimal control. The technology is currently used in a dry ESP and can next be studied for a wet ESP.
- (2) Researching the regulation technology to realize the overall optimal energy consumption by combining it with denitrification and desulfurization.

4. Conclusions

This paper proposes an optimization method for an ESP, establishes a voltage-current characteristic model, an outlet dust concentration prediction model, and a PSO model. Finally, the optimization experiment is conducted in a 330 MW power plant to validate the proposed model, and the following conclusions can be drawn:

- (1) The voltage-current characteristic model is constructed through the charging mechanism and parameter correction, then the model is trained by historical data. The results show the performance is excellent, with a MAPE of 1.5% and a RRMSE of 1.8%.
- (2) The outlet dust concentration prediction model is constructed based on the mechanism model and the data model. The RRMSE of the training set and testing set are 1.8% and 6.9%, the MAPE are 1.4% and 5.2%, and an accurate prediction of the outlet dust concentration has been achieved.
- (3) The PSO is used to obtain the optimal secondary voltage, which can minimize the power consumption of the ESP while meeting the outlet dust concentration requirement.
- (4) Compared to the manual control, the energy saving is about 43% after the PSO control, with an annual average carbon reduction of approximately 2621.34 t, and the fluctuation of the outlet dust concentration is more stable.

Author Contributions: Conceptualization, J.Z.; Methodology, C.F.; Software, Z.Z.; Validation, C.F. and H.Y.; Formal analysis, C.F.; Data curation, C.F. and Y.L.; Writing—original draft preparation, J.Z.; Writing—review and editing, C.F.; Supervision, J.Z. All authors have read and agreed to the published version of the manuscript.

Funding: This research received no external funding.

Data Availability Statement: The data used to support the findings of this study are available from the corresponding author upon request.

Conflicts of Interest: Author Jianjun Zhu, Chao Feng, Haoming Yang and Yujie Liu were employed by the company Zhejiang Doway Advanced Technology Co., Ltd. The remaining authors declare that the research was conducted in the absence of any commercial or financial relationships that could be construed as a potential conflict of interest.

References

1. Huang, X. *Annual Development Report on World Energy (2022)*; Social Science Academic Press: Beijing, China, 2022.
2. Tang, J.; Wang, J. Coal development and countermeasures under the carbon peaking and carbon neutrality goals. *China Mining Mag.* **2023**, *32*, 22–31.
3. Guo, H.N.; Wu, Y.; Wang, X.B.; Zhang, M.; Huang, Z. Current status of power generation technology of the agriculture and forest biomass co-firing in coal—Fired power plants. *Clean Coal Technol.* **2022**, *28*, 12–22.
4. Yang, M.L.; Sun, L.J.; Dai, B.; Wu, W.L.; Cai, M.; Li, S. Research on mixed coals combustion strategy of thermal power unit based on deep peak shaving. *Coal Quality Technol.* **2022**, *37*, 46–51.

5. Shuai, Y.; Zhao, B.; Jiang, D.F.; He, S.Y.; Lyu, J.F.; Yue, G.Y. Status and prospect of coal-fired high efficiency and clean power generation technology in China. *Therm. Power Gener.* **2022**, *51*, 1–10.
6. Ma, S.C.; Fan, S.J.; Wu, K.; Yang, P.W.; Chen, L.T. CCUS technology development of coal-fired power plant under the back ground of Dual Carbon Strategy: Challenges and countermeasures. *Clean Coal Technol.* **2022**, *28*, 1–13.
7. Liu, H.X. Energy saving and carbon reduction analysis of electrostatic precipitator under double carbon background. *Power Gener. Tech.* **2023**, *44*, 738–744.
8. Liu, H.X.; Li, J.G.; Yao, Y.P.; Zhong, J.F.; Du, Y.J.; Du, Y.Q. Evaluation on the energy efficiency of electrostatic precipitators in coal-fired power plants. *Electr. Power* **2017**, *50*, 22–27.
9. Li, W.H.; Bai, L.; Yu, S.C. Numerical simulation of flow field particle field and electric field for ESP. *Power Gener. Tech.* **2021**, *42*, 336–342.
10. Wang, Z.G.; Zhang, C.; Li, D.Y.; Bai, Y.G.; Chen, J.Y. Experiment of energy saving and optimization on electrostatic precipitator system in ultra-low emission coal-fired power plants. *Therm. Power Gener.* **2018**, *47*, 109–114.
11. Li, D.Z.; Tian, L.; Liu, S.P.; Wang, R. Optimized control of the working voltage for electrostatic precipitator based on intellectual method. *Energy Conserv. Technol.* **2006**, *24*, 538–541.
12. Chen, W.G. Mathematical Model and Fuzzy Multi-objec Optimization Design of Electrostatic Precipitator. Master's Thesis, Zhejiang University, Hangzhou, China, 2006.
13. Grass, N.; Zintl, A.; Hoffmann, E. Electrostatic Precipitator Control Systems. *IEEE Ind. App. Mag.* **2010**, *16*, 28–33. [[CrossRef](#)]
14. Liu, X.P.; Li, Q.Y.; Li, D.Y.; Guo, M.; Li, J.G. Energy-saving optimization on the dust collection system of a 330 MW power plant. *Electr. Power* **2019**, *52*, 165–169.
15. Li, D.Z.; Tian, L.; Zhang, Z.W.; Liu, S.P. The causes of efficiency decrease for boiler electrostatic precipitator and its improvements. *Ind. Sfty. Environ. Prot.* **2005**, *31*, 32–34.
16. Yang, Z.D. Mechanism and Application for Simultaneous Removal of PM and SO_x from Wet Flue Gas Enhanced by External Fields. Ph.D. Thesis, Zhejiang University, Hangzhou, China, 2018.
17. Cooperman, G. A New Current-Voltage Relation for Duct Precipitators Valid for Low and High Current Densities. *IEEE Trans. Ind. Appl* **1981**, *IA-17*, 236–239. [[CrossRef](#)]
18. Guo, Y.S. Mechanism and Application for Modeling and Coordinated High Efficiency Removal of PM/SO₃ in Coal Fired Flue Gas. Ph.D. Thesis, Zhejiang University, Hangzhou, China, 2020.
19. Deutsch, W. Clean Coal Technology Bewegung und Ladung der Elektrizitätsträger in Zylinderkondensator. *Ann. Der Phys.* **1922**, *373*, 335–344. [[CrossRef](#)]
20. Li, D.Y.; Liu, X.P.; Zhang, C. Correction of the dust removal efficiency formula on low-low temperature electrostatic precipitator. *Proc. CSEE* **2022**, *42*, 2623–2629.
21. Luong, T.; Pham, H.; Manning, C.D. Effective Approaches to Attention-based Neural Machine Translation. *arXiv* **2015**, arXiv:1508.04025. [[CrossRef](#)]
22. Huang, Y.Q. Research on Simultaneous Removal of Multi-pollutants and Global Optimization for Ultra-low Emission System in Coal-fired Unit. Master's Thesis, Zhejiang University, Hangzhou, China, 2020.

Disclaimer/Publisher's Note: The statements, opinions and data contained in all publications are solely those of the individual author(s) and contributor(s) and not of MDPI and/or the editor(s). MDPI and/or the editor(s) disclaim responsibility for any injury to people or property resulting from any ideas, methods, instructions or products referred to in the content.